Modeling and simulation of 5-axis milling processes

E. Budak (2)*, E. Ozturk, L.T. Tunc

Faculty of Engineering and Natural Sciences, Sabanci University, Istanbul, Turkey

ARTICLE INFO

Keywords:
Milling
Force
Stability

ABSTRACT

5-axis milling is widely used in machining of complex surfaces. Part quality and productivity are extremely important due to the high cost of machine tools and parts involved. Process models can be used for the selection of proper process parameters. Although extensive research has been conducted on milling process modeling, very few are on 5-axis milling. This paper presents models for 5-axis milling process geometry, cutting force and stability. The application of the models in selection of important parameters is also demonstrated. A practical method, developed for the extraction of cutting geometry, is used in simulation of a complete 5-axis cycle.

1. Introduction

5-axis milling has become a widely used process due to its ability to machine complex surfaces. In most of these applications high productivity is required due to the cost of machine tools and parts. Productivity and quality in 5-axis milling can be increased using process models. However, unlike other processes, modeling of 5-axis milling has been very limited. The objective of this paper is to demonstrate selection of process parameters in 5-axis milling for increased productivity using process models and simulations.

Altintas and Engin [1] modeled the cutting edge for generalized milling cutters, and used it in cutting force and stability calculations in 3-axis milling which can be extended to 5-axis milling. However, all process models require tool–part engagement boundaries which are more complicated in 5-axis milling due to the additional degrees of freedom. The calculation of engagement limits in 5-axis milling has been mainly done using non-analytical methods. For example, Larue and Altintas [2] used ACIS [3] solid modeling environment to determine the engagement region for force simulations of flank milling. Kim et al. [4] determined the engagement region using Z-mapping. Ozturk and Budak [5], on the other hand, determined the engagement regions analytically, and modeled the cutting forces and tool deflections.

Chatter is one of the main limitations in 5-axis milling. Although chatter stability in milling has been extensively studied analytically [6–8] and by simulations [9], this has been very limited for ball-end milling and 5-axis milling processes. Altintas et al. [10] extended the analytical milling stability model to the ball-end milling whereas Ozturk and Budak [11,12] included the effect of lead and tilt angles using single- and multi-frequency methods.

Force and the stability models can be used both in planning and analysis. In planning phase, better process parameters can be selected through simulations. In 5-axis milling, however, process parameters may continuously vary along the tool path. In this study, these parameters are obtained using a procedure [13] developed for extraction of milling conditions from cutter location (CL) data. As all CAD/CAM software provides CL files, this approach presents a practical method for integration of the models with the CAD/CAM systems.

In the next section, the geometry of 5-axis milling is briefly introduced together with the force model. The application of the model in lead and tilt angle selection is also demonstrated. For chatter stability analysis of 5-axis milling, single- and multi-frequency solutions are summarized, and used for generation of stability diagrams. The last section of the paper presents simulation of 5-axis milling cycles with example cases.

2. Process geometry and force model

Compared with conventional milling operations, 5-axis milling geometry is more complicated due to the additional degrees of freedom. In this section, 5-axis milling geometry is presented briefly. A more detailed analysis can be found in [5]. Three coordinate systems are used in modeling of 5-axis milling processes. MCS is a fixed coordinate system on the machine tool. TCS consists of the tool axis and two perpendicular transversal axes (x) and (y). FCN consists of the feed, F, the surface normal, N and the cross-feed, C, directions (Fig. 1). The lead angle is the rotation of the tool axis about the cross-feed axis, whereas the tilt angle is the rotation about the feed axis with respect to the surface normal. Lead and tilt angles together with ball-end mill geometry, cutting depth and step over determine the engagement region between the cutting tool and workpiece. In Fig. 1, engagement region, variation of start (φ_{st}) and exit angles (φ_{ex}) along the tool axis are demonstrated for a representative case.

The cutting tool is divided into differential cutting elements to determine the varying engagement boundaries (Fig. 1). The engagement model [5] is used to determine the elements that are in cut. Differential cutting forces in radial, tangential and axial directions shown in Fig. 2 are calculated in terms of the local chip thickness and width, and the local cutting force coefficients. Local chip thickness and cutting force coefficients are variable along the cutting flute depending on the immersion angle φ and z coordinate as presented in Fig. 3.

* Corresponding author.

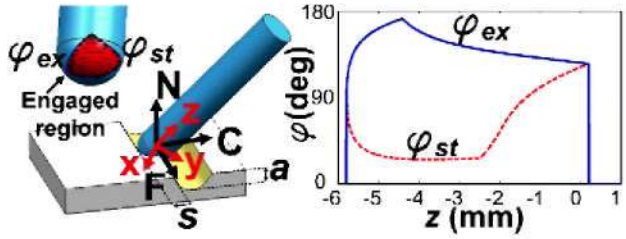

Fig. 1. Engagement region, start and exit angles.

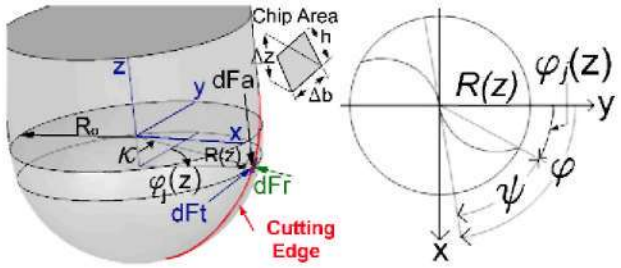

Fig. 2. Tool geometry and differential cutting forces.

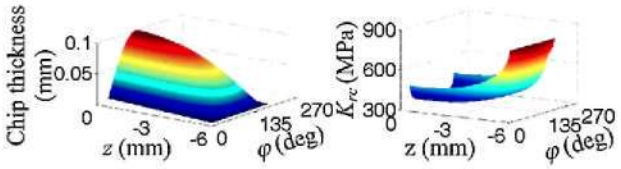

Fig. 3. Chip thickness and force coefficient variation.

Cutting forces, torque and power are calculated by integrating the differential forces within the engagement region. Tool deflections are calculated using the structural properties of the cutting tool and forces at surface generation points [5].

2.1. Force model results

The force model was verified with more than 70 cutting tests [5]. The force model can be used in the selection of lead and tilt angles. The effect of lead and tilt angles on the maximum transversal cutting force, F_{xy}^{max}, is simulated for a representative following-cut case in Fig. 4. The cutting depth and the step over are 5 mm, the feed rate is 0.05 mm/tooth, the spindle speed is 1000 rpm and cross-feed direction [5] is negative. A 12 mm-diameter, two-fluted ball-end mill with 30° helix and 8° rake angle is used. The workpiece material is Ti6Al4V which is commonly used in aerospace industry. Three different lead and tilt combinations are selected in Fig. 4, and the simulations are verified by cutting tests. Comparison of measured and simulated F_{xy}^{max} is given in Fig. 4. The variation of measured and simulated cutting forces in x, y and z directions for one revolution of

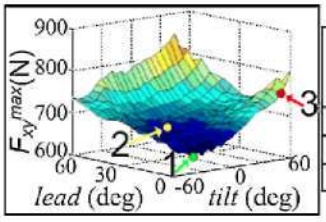

Point	Lead,tilt (deg)	Sim. F_{xy}^{max} (N)	Meas. F_{xy}^{max} (N)
1	0, -40	637	600
2	30, -15	672	652
3	0, 50	752	712

Fig. 4. Simulated and measured cutting forces.

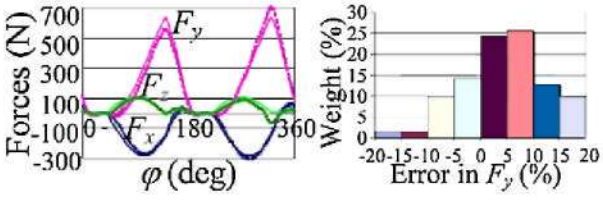

Fig. 5. Predicted forces and error distribution.

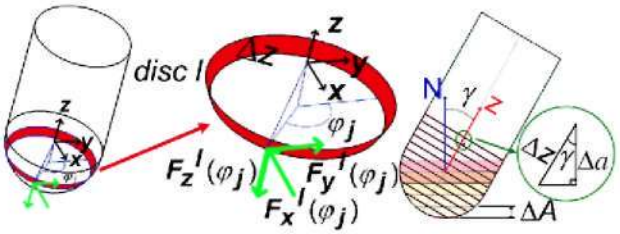

Fig. 6. Dynamic forces on the disc element l.

the tool is given in Fig. 5 for the data point 2. The full curves represent simulation results whereas curves with markers are experimental measurements. It is seen that the model predictions are in good agreement with the measurements. Distribution of the prediction error for all tests is demonstrated in Fig. 5.

3. Stability model

In the stability model, the variations of engagement and cutting conditions are taken into account by dividing the tool into disc elements with thickness of Δz (Fig. 6). The dynamic cutting forces in x, y and z directions for reference immersion angle φ on a disc element l is calculated as follows:

$$[F_x^l(\varphi) F_y^l(\varphi) F_z^l(\varphi)]^T = \Delta a \boldsymbol{B}^l(\varphi)\boldsymbol{d} \tag{1}$$

where Δa is the height of the disc elements in surface normal direction, $\boldsymbol{B}^l(\varphi)$ is the lth disc's directional coefficient matrix [8] at the reference immersion angle φ. $\boldsymbol{d}$ is the dynamic displacement vector which can be expressed as the difference between the displacements at current time and one tooth period before (Fig. 7):

$$\boldsymbol{d} = [x(t) - x(t-\tau) \quad y(t) - y(t-\tau) \quad z(t) - z(t-\tau)]^T \tag{2}$$

where τ is the tooth period. As the reference immersion angle is dependent on time, $\boldsymbol{B}^l(\varphi)$ is a time dependent periodic directional coefficient matrix. It can be represented by Fourier series expansion as follows [8]:

$$\boldsymbol{B}^l(\varphi) = \sum_{r=-\infty}^{r=\infty} \boldsymbol{B}_r^l e^{ir\varphi}, \boldsymbol{B}_r^l = \frac{1}{\varphi_p}\int_0^{\varphi_p} \boldsymbol{B}^l(\varphi) e^{-ir\varphi} d\varphi \tag{3}$$

Depending on the Fourier series expansion of the directional coefficients, there are two different stability formulation methods [8]. In the single-frequency solution, only the average of the directional coefficient matrix is used whereas in multi-frequency solution directional coefficient matrix is represented by more than one term.

3.1. Single-frequency solution

In single-frequency solution, the dynamic displacement vector is assumed to be composed of only chatter frequency ω_c. Then, it can be defined in terms of the transfer function of the structure and cutting forces [11]:

$$\boldsymbol{d} = (1 - e^{-i\omega_c\tau})\boldsymbol{G}(i\omega_c)[F_x(t) \quad F_y(t) \quad F_z(t)]^T \tag{4}$$

where $F_x(t)$, $F_y(t)$, $F_z(t)$ are total dynamic cutting forces and $\boldsymbol{G}$ is the transfer function in TCS. If Eq. (1) is written for m disc elements and summed where Eq. (4) is substituted for the dynamic displacement vector, the following eigenvalue problem is obtained:

$$[\boldsymbol{F}]e^{i\omega_c t} = \Delta a(1 - e^{-i\omega_c\tau})\left(\sum_{l=1}^{m}\boldsymbol{B}_0^l\right)\boldsymbol{G}(i\omega_c)[\boldsymbol{F}]e^{i\omega_c t} \tag{5}$$

Since the number of disc elements to be included in the analysis is not known, stability diagrams are obtained using an iterative procedure [12].

In 3-axis flat end milling, it was shown that the single-frequency solution gives good results except low radial immersion with respect to the tool diameter. However, for low radial immersion, stability diagrams were shown to be affected by multi-frequency effects [14].

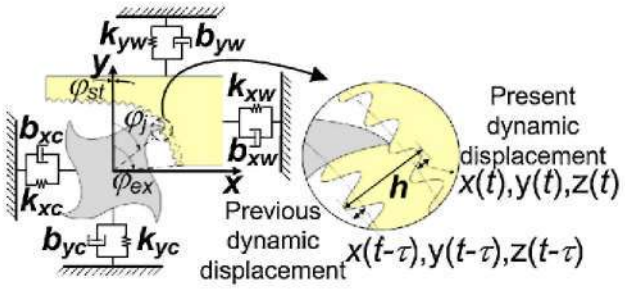

Fig. 7. The dynamic chip thickness.

3.2. Multi-frequency solution

In multi-frequency solution, higher order terms are included in the representation of directional coefficients. Multiple frequencies are addition and subtraction of the chatter frequency and harmonics of the tooth passing frequency. In this case, the dynamic displacement vector in TCS can be written in terms of the transfer function $\boldsymbol{G}$ and total dynamic cutting forces [15]:

$$\boldsymbol{d} = (1 - e^{-i\omega_c \tau}) \sum_{k=-\infty}^{k=\infty} \boldsymbol{G}(i\omega_c + ik\omega_t)\boldsymbol{F}_k e^{i(i\omega_c + k\omega_t)t} \tag{6}$$

As performed in the single-frequency solution, Eq. (1) is summed side by side for all disc elements and Eq. (6) is substituted for the dynamic displacement vector. The resulting eigenvalue problem depends on both chatter and tooth passing frequencies unlike the single-frequency solution. The numerical multi-frequency solution to obtain stability diagrams is presented in [12].

5-axis milling is used especially in finishing operations where radial depth, i.e. step over, is low. Hence, one would expect to see significant multi-frequency effects on the stability diagrams based on the observations from flat-end milling [14]. However, due to the effect of lead and tilt angles and ball-end mill geometry, these affects are suppressed in 5-axis milling. This is due to the fact that the ratio of time spent in cutting to non-cutting in 5-axis milling is higher with respect to flat-end milling. This is demonstrated in [12] by comparing the directional coefficients for flat-end milling and for ball-end milling.

3.3. Effect of machine tool kinematics configuration

The feed direction may have effect on the chatter stability if the transfer functions in two orthogonal directions are not equal. For machine tool configurations, where the rotary motions are on the tool side, lead and tilt angles do not affect the feed direction. However, if the rotary axes are on the table side, the feed vector with respect to an inertial reference frame (i.e. MCS) may become dependent on lead and tilt angles (Fig. 8a). For these cases, the measured transfer functions must be oriented considering the feed direction. The orientation of a measured transfer function $\boldsymbol{H}(i\omega_c)$ is performed using $\boldsymbol{T}_G$ matrix which depends on the lead and tilt angles, and orientation of FCN with respect to MCS [12]:

$$\boldsymbol{G} = \boldsymbol{T}_G^T \boldsymbol{H} \boldsymbol{T}_G \tag{7}$$

3.4. Stability model results

The results of the stability model are presented for a case where the workpiece material AISI 1050 steel is slotted using a 20 mm diameter ball-end mill. The modal data measured at the tool tip is given in Table 1. Firstly, the effects of lead and tilt angles on the absolute stability limit using the single-frequency method are demonstrated in Fig. 8b. For 3 lead and tilt angle combinations experimentally determined absolute stability limits are also shown. For the lead and tilt combination of (15°, −15°), the stability diagrams using single-frequency and multi-frequency methods were generated. It was observed that the measured chatter frequencies were lower than the predicted ones. This can be due to the fact that the most flexible mode presented in Table 1 is the spindle mode which was measured in idle condition, but the modal frequencies of the spindle may shift during cutting. Based on this observation, the measured frequencies under static conditions were modified in the simulations in order to match the measured chatter frequencies with the predicted ones. The simulation results using unmodified modal data with single-frequency method (hk0), modified modal data with single-frequency method (hk0_mod) and with multi-frequency method with one harmonics (hk1_mod) are presented in Fig. 9. It is seen that the simulated stability diagrams agree better with the experimental results after modified modal data is used. Furthermore, it was observed that using higher harmonics did not change the simulated stability diagrams. For the modified modal data, a time-domain model [12] was run at several spindle speeds and corresponding stability limits are presented in Fig. 9. The power spectrum of the simulated displacements is used to judge the stability of the system. There is some discrepancy between frequency-domain and time-domain results which can be attributed to the discretization procedure employed. At a stable point (A) and at an unstable point (B), power spectrums of cutting tool displacements predicted by the time-domain model are presented in Fig. 9 to be representative.

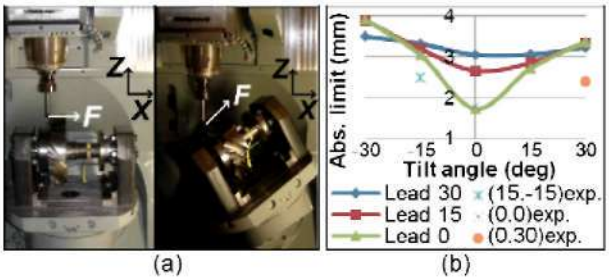

Fig. 8. Effect of lead, tilt angles on feed direction and stability.

Table 1
Modal data for the example case.

Direction	f_n (Hz)	ζ (%)	k (N/mm)
X	747.3	3.89	26,300
Y	766	3.98	36,000

4. Process simulation

For simulations, cutting geometry and conditions must be known whereas they, in general, vary continuously in 5-axis milling cycles. A practical method has been developed [13], and it is briefly described here, for identification of these parameters to simulate a full cycle.

4.1. Identification of cutting conditions

In this approach, tool orientation and position are directly obtained from the cutter location (CL) file whereas geometrical parameters, i.e. cutting depth, step over, lead and tilt angles are

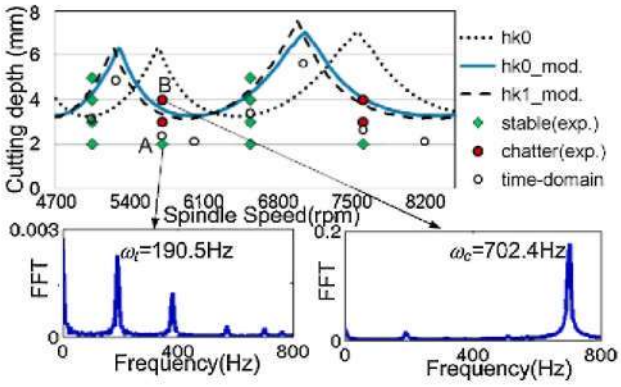

Fig. 9. Stability diagram for (15°, −15°) combination.